

Electroweak Symmetry Non-restoration in UV-complete Models with New Fermions

Yu Hang Ng

Department of Physics and Astronomy
University of Nebraska-Lincoln

APS Division of Particles & Fields Meeting
July 14, 2021

INTRODUCTION

Electroweak symmetry is restored at high temperature in Standard Model and most of the BSM theories. For examples,

1. SM:

$$\left. \frac{\partial^2 V_1^{th}}{\partial h^2} \right|_{h=0} = T^2 \left(\frac{3}{16} g^2 + \frac{1}{16} g'^2 + \frac{1}{4} \lambda_t^2 + \frac{1}{2} \lambda \right)$$

2. SM + real singlet scalar (\mathbb{Z}_2):

$$\left. \frac{\partial^2 V_1^{th}}{\partial h^2} \right|_{h=0} = T^2 \left(\frac{3}{16} g^2 + \frac{1}{16} g'^2 + \frac{1}{4} \lambda_t^2 + \frac{1}{2} \lambda + \frac{1}{12} \lambda_{hs} \right)$$

EWSNR VIA NEW SCALARS

In some models, Electroweak symmetry was always broken (SNR) or only temporary restored (TR).

1. SM + singlet scalar s_i with $O(N_s)$ global symmetry (Meade & Ramani, 1807.07578):

$$V = V_{SM} + \frac{1}{2}\mu_s^2(s_i s_i) + \frac{1}{4}\lambda_s(s_i s_i)^2 + \frac{1}{2}\lambda_{hs}h^2(s_i s_i)$$

$$\left. \frac{\partial^2 V_1^{th}}{\partial h^2} \right|_{h=0} = T^2 \left(\frac{3}{16}g^2 + \frac{1}{16}g'^2 + \frac{1}{4}\lambda_t^2 + \frac{1}{2}\lambda + \frac{N_s}{12}\lambda_{hs} \right)$$

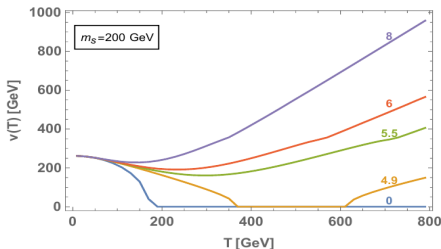
EWSNR VIA NEW SCALARS

In some models, Electroweak symmetry was always broken (SNR) or only temporary restored (TR).

1. SM + singlet scalar s_i with $O(N_s)$ global symmetry (Meade & Ramani, 1807.07578):

$$V = V_{SM} + \frac{1}{2}\mu_s^2(s_i s_i) + \frac{1}{4}\lambda_s(s_i s_i)^2 + \frac{1}{2}\lambda_{hs}h^2(s_i s_i)$$

$$\left. \frac{\partial^2 V_1^{th}}{\partial h^2} \right|_{h=0} = T^2 \left(\frac{3}{16}g^2 + \frac{1}{16}g'^2 + \frac{1}{4}\lambda_t^2 + \frac{1}{2}\lambda + \frac{N_s}{12}\lambda_{hs} \right)$$



Temperature dependent vev for different values of $N_s |\lambda_{hs}|$.

EWSNR VIA NEW SCALARS

In some models, Electroweak symmetry was always broken (SNR) or only temporary restored (TR).

1. SM + singlet scalar s_i with $O(N_s)$ global symmetry (Meade & Ramani,1807.07578):

$$V = V_{SM} + \frac{1}{2}\mu_s^2(s_i s_i) + \frac{1}{4}\lambda_s(s_i s_i)^2 + \frac{1}{2}\lambda_{hs}h^2(s_i s_i)$$

$$\left. \frac{\partial^2 V_1^{th}}{\partial h^2} \right|_{h=0} = T^2 \left(\frac{3}{16}g^2 + \frac{1}{16}g'^2 + \frac{1}{4}\lambda_t^2 + \frac{1}{2}\lambda + \frac{N_s}{12}\lambda_{hs} \right)$$

2. SM + Inert Higgs Doublet + singlet scalar($O(N_s)$) (Carena et al.,2104.00638)
3. 2HDM + real singlet scalar (Heinemeyer et at.,2103.12707)

EWSNR VIA NEW SCALARS

In some models, Electroweak symmetry was always broken (SNR) or only temporary restored (TR).

1. SM + singlet scalar s_i with $O(N_s)$ global symmetry (Meade & Ramani, 1807.07578):

$$V = V_{SM} + \frac{1}{2}\mu_s^2(s_i s_i) + \frac{1}{4}\lambda_s(s_i s_i)^2 + \frac{1}{2}\lambda_{hs}h^2(s_i s_i)$$

$$\left. \frac{\partial^2 V_1^{th}}{\partial h^2} \right|_{h=0} = T^2 \left(\frac{3}{16}g^2 + \frac{1}{16}g'^2 + \frac{1}{4}\lambda_t^2 + \frac{1}{2}\lambda + \frac{N_s}{12}\lambda_{hs} \right)$$

2. SM + Inert Higgs Doublet + singlet scalar ($O(N_s)$) (Carena et al., 2104.00638)
3. 2HDM + real singlet scalar (Heinemeyer et al., 2103.12707)

Is it possible to achieve SNR or TR for EW symmetry by adding **new fermions** to SM?

EWSNR VIA NEW FERMIONS

In high temperature limit (i.e. when $m_i^2 \ll T^2$), (Matsedonskyi, Servant, 2002.05174)

$$\begin{aligned} \left. \frac{\partial^2 V_{1,F}^{th}}{\partial h^2} \right|_{h=0} &= \sum_i T^2 \frac{n_F}{48} \frac{\partial^2 m_i^2}{\partial h^2} = T^2 \frac{n_F}{48} \frac{\partial^2}{\partial h^2} \sum_i m_i^2 \\ &= T^2 \frac{n_F}{48} \frac{\partial^2}{\partial h^2} \text{Tr}(M_f^\dagger M_f) = T^2 \frac{n_F}{48} \frac{\partial^2}{\partial h^2} \sum_{i,j} |M_{ij}|^2 \end{aligned}$$

In renormalizable models, $M_{ij} = a_0 + a_1 h$, hence $\left. \frac{\partial^2 V_{1,F}^{th}}{\partial h^2} \right|_{h=0} \geq 0$. Thus, it is impossible to achieve EWSNR by adding new fermions!

SINGLET-DOUBLET MODEL

$$L_{L,R} = \begin{bmatrix} N \\ E \end{bmatrix}_{L,R} \sim (1, 2)_{-\frac{1}{2}}, \quad N'_{L,R} \sim (1, 1)_0$$

$$\begin{aligned} \mathcal{L}_{mass}^i &= -y_1 \overline{L}_L \tilde{\phi} N'_R - y_2 \overline{N}'_L \tilde{\phi}^\dagger L_R - m_L \overline{L}_L L_R - m_{N'} \overline{N}'_L N'_R + h.c. \\ &= -\overline{F}_L M F_R \end{aligned}$$

$$F_{L,R} = \begin{bmatrix} N' \\ N \\ E \end{bmatrix}, \quad M = \begin{bmatrix} m_{N'} & m_{NN'2} & 0 \\ m_{NN'1} & m_L & 0 \\ 0 & 0 & m_L \end{bmatrix}, \quad m_{NN'i} = y_i h / \sqrt{2},$$

$$\phi = \begin{bmatrix} G^+ \\ (h + iG^0) / \sqrt{2} \end{bmatrix}, \quad \tilde{\phi} = i\sigma_2 \phi^*.$$

The mass matrix can be diagonalized by biunitary transformation. The physical masses are m_L, m_{N1}, m_{N2} .

$$m_{N1}^2 = \frac{1}{2} \left(A_N^2 - \sqrt{(A_N^2)^2 - 4(\Delta_N^2)^2} \right)$$
$$m_{N2}^2 = \frac{1}{2} \left(A_N^2 + \sqrt{(A_N^2)^2 - 4(\Delta_N^2)^2} \right)$$

where

$$A_N^2 = |m_{NN'1}|^2 + |m_{NN'2}|^2 + |m_{N'}|^2 + |m_L|^2$$
$$\Delta_N^2 = |m_L m_{N'} - m_{NN'1} m_{NN'2}|$$

$$\left. \frac{\partial^2 V_{1,F}^{th}}{\partial h^2} \right|_{h=0} = \frac{T^2}{12} \frac{\partial^2}{\partial h^2} \sum_{N1, N2, L} m_i^2 > 0$$



What if the heavier fermion (N_2) is decoupled from the thermal bath?

When $m_L^2 \gg m_{N'}^2$, $\frac{1}{2}|y_1 y_2| h^2$, T^2 ,

$$m_{N1}^2 \approx m_{N'}^2 - \frac{m_{N'} \operatorname{Re}(y_1 y_2)}{m_L} h^2, \quad m_{N2}^2 \approx m_L^2 + \frac{m_{N'} \operatorname{Re}(y_1 y_2)}{m_L} h^2$$

$$\left. \frac{\partial^2 V_{1,F}^{th}}{\partial h^2} \right|_{h=0} = \frac{T^2}{12} \frac{\partial^2}{\partial h^2} m_{N1}^2 = -\frac{T^2}{6} \frac{m_{N'} \operatorname{Re}(y_1 y_2)}{m_L}$$

Thus, $\left. \frac{\partial^2 V_{1,F}^{th}}{\partial h^2} \right|_{h=0} < 0$ is possible by choosing $\operatorname{Re}(y_1 y_2) > 0$.

$m_L^2 \gg T^2$ is possible if new fermions gain their masses through some dynamical mechanism.

MODEL I: SINGLET-DOUBLET FERMIONS

+ REAL SCALAR SINGLET + SCALAR SINGLET WITH $O(N_\rho)$

$$L_{L,R}^i = \begin{bmatrix} N^i \\ E^i \end{bmatrix}_{L,R} \sim (1, 2)_{-\frac{1}{2}}, \quad N_{L,R}^{\prime i} \sim (1, 1)_0, \quad E_{L,R}^{\prime i} \sim (1, 1)_{-1}$$

$$\mathcal{L} = \mathcal{L}_{SM} + \sum_{i=1}^{N_F} (\mathcal{L}_{kin}^i(L, N', E') + \mathcal{L}_{yuk}^i) + \mathcal{L}_{kin}(\sigma, \rho) - V_0(\sigma, \rho)$$

$$\begin{aligned} \mathcal{L}_{yuk}^i = & -y_{NN'1}^i \bar{L}_L^i \tilde{\phi} N_R^{\prime i} - y_{NN'2}^i \bar{N}_L^{\prime i} \tilde{\phi}^\dagger L_R^i - y_{EE'1}^i \bar{L}_L^i \phi E_R^{\prime i} - y_{EE'2}^i \bar{E}_L^{\prime i} \phi^\dagger L_R^i \\ & - y_L^i \sigma \bar{L}_L^i L_R^i - y_{N'}^i \sigma \bar{N}_L^{\prime i} N_R^{\prime i} - y_{E'}^i \sigma \bar{E}_L^{\prime i} E_R^{\prime i} + h.c. \end{aligned}$$

$$\begin{aligned} V_0(\sigma, \rho) = & -\frac{1}{2} \mu_\sigma^2 \sigma^2 + \frac{1}{4} \lambda_\sigma \sigma^4 \\ & -\frac{1}{2} \mu_\rho^2 \rho_i \rho_i + \frac{1}{4} \lambda_\rho (\rho_i \rho_i)^2 + \frac{1}{4} \lambda_{\sigma\rho} \sigma^2 \rho_i \rho_i \end{aligned}$$

The physical masses (for each copy of new fermions) are:

$$m_{N1}^2 = \frac{1}{2} \left(A_N^2 - \sqrt{(A_N^2)^2 - 4(\Delta_N^2)^2} \right)$$

$$m_{N2}^2 = \frac{1}{2} \left(A_N^2 + \sqrt{(A_N^2)^2 - 4(\Delta_N^2)^2} \right)$$

where

$$A_N^2 = |m_{NN'1}|^2 + |m_{NN'2}|^2 + |m_{N'}|^2 + |m_L|^2$$

$$\Delta_N^2 = |m_L m_{N'} - m_{NN'1} m_{NN'2}|$$

$$m_{NN'i} = \frac{1}{\sqrt{2}} y_{NN'i} h, \quad (i = 1, 2)$$

$$m_x = y_x \sigma, \quad (x = L, N', E')$$

m_{E1}, m_{E2} are same as equations above, except $N \rightarrow E$.

At high T, when $(y_L v_\sigma)^2 \gg T^2$,

$$\begin{aligned}\partial_h^2 V_1^{th}(h=0, v_\sigma) &= -a_h T^2, \\ a_h &= \frac{N_F}{6y_L} (y_{N'} y_{NN'1} y_{NN'2} + y_{E'} y_{EE'1} y_{EE'2}) \\ &\quad - \left(\frac{3}{16} g^2 + \frac{1}{16} g'^2 + \frac{1}{4} y_i^2 + \frac{1}{2} \lambda_h \right).\end{aligned}$$

- When $\frac{N_F}{6y_L} (y_{N'} y_{NN'1} y_{NN'2} + y_{E'} y_{EE'1} y_{EE'2})$ is large enough, the negative contribution outweighs the usual positive contributions from SM particles, thus $\partial_h^2 V_{eff}(h=0, v_\sigma) < 0$, and $v_h \neq 0$ at high T.

$$\partial_{\sigma}^2 V_1^{th}(h=0, \sigma=0) = -a_{\sigma} T^2,$$
$$a_{\sigma} = -\frac{N_{\rho}}{24} \lambda_{\sigma\rho} - \frac{1}{4} \lambda_{\sigma} - \frac{N_F}{6} \left(2y_L^2 + y_{N'}^2 + y_{E'}^2 \right).$$

- To satisfy $(y_L v_{\sigma})^2 \gg T^2$, we need large enough v_{σ} at high T too.
- $a_{\sigma} > 0$ guarantees that $v_{\sigma} \neq 0$ at high T. Although this condition is neither sufficient nor necessary, it helps us to obtain the correct benchmarks.
- $\lambda_{\sigma\rho} < 0$ and sufficiently large $N_{\rho} |\lambda_{\sigma\rho}|$ are required to satisfy $a_{\sigma} > 0$.

MODEL II: SINGLET-DOUBLET FERMIONS

+ REAL SCALAR SINGLET + SCALAR SINGLET WITH $O(N_\rho)$ + INERT HIGGS
DOUBLET

$$V_0 = V_0(\Phi_1, \Phi_2) + V_0(\sigma, \rho) + \tilde{V}_0$$

$$V_0(\Phi_1, \Phi_2) = -\mu_1^2 \Phi_1^\dagger \Phi_1 + \lambda_1 \left(\Phi_1^\dagger \Phi_1 \right)^2 - \mu_2^2 \Phi_2^\dagger \Phi_2 + \lambda_2 \left(\Phi_2^\dagger \Phi_2 \right)^2$$

$$\tilde{V}_0 = \lambda_3 (\Phi_1^\dagger \Phi_1) (\Phi_2^\dagger \Phi_2) + \lambda_4 (\Phi_1^\dagger \Phi_2) (\Phi_2^\dagger \Phi_1)$$

$$+ \sum_{i=1}^2 \left(\frac{1}{2} \lambda_{\sigma\Phi_i} \sigma^2 (\Phi_i^\dagger \Phi_i) + \frac{1}{2} \lambda_{\rho\Phi_i} (\rho_j \rho_j) (\Phi_i^\dagger \Phi_i) \right)$$

$$\begin{aligned} \mathcal{L}_{yuk}^i = & -y_{NN'1}^i \overline{L}_L^i \widetilde{\Phi}_2 N_R^{i'} - y_{NN'2}^i \overline{N}_L^{i'} \widetilde{\Phi}_2^\dagger L_R^i - y_{EE'1}^i \overline{L}_L^i \Phi_2 E_R^{i'} - y_{EE'2}^i \overline{E}_L^{i'} \Phi_2^\dagger L_R^i \\ & - y_L^i \sigma \overline{L}_L^i L_R^i - y_{N'}^i \sigma \overline{N}_L^{i'} N_R^{i'} - y_{E'}^i \sigma \overline{E}_L^{i'} E_R^{i'} + h.c. \end{aligned}$$

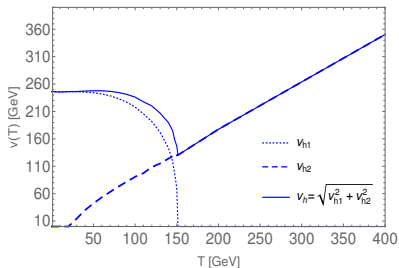
$$\begin{aligned} a_h = & \frac{N_F}{6y_L} (y_{N'} y_{NN'1} y_{NN'2} + y_{E'} y_{EE'1} y_{EE'2}) \\ & - \left(\frac{3}{16} g^2 + \frac{1}{16} g'^2 + \frac{1}{2} \lambda_2 \right) \end{aligned}$$

At $T = 0$,

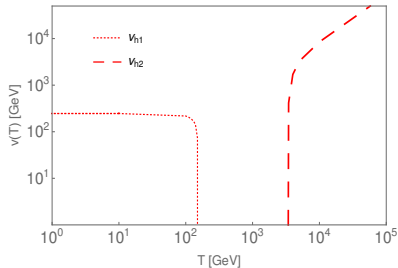
$$\Phi_j = \begin{bmatrix} \varphi_j^+ \\ (h_j + i\varphi_j^0)/\sqrt{2} \end{bmatrix}$$

$$\langle \Phi_2 \rangle = \begin{bmatrix} 0 \\ 0 \end{bmatrix}$$

THERMAL HISTORIES

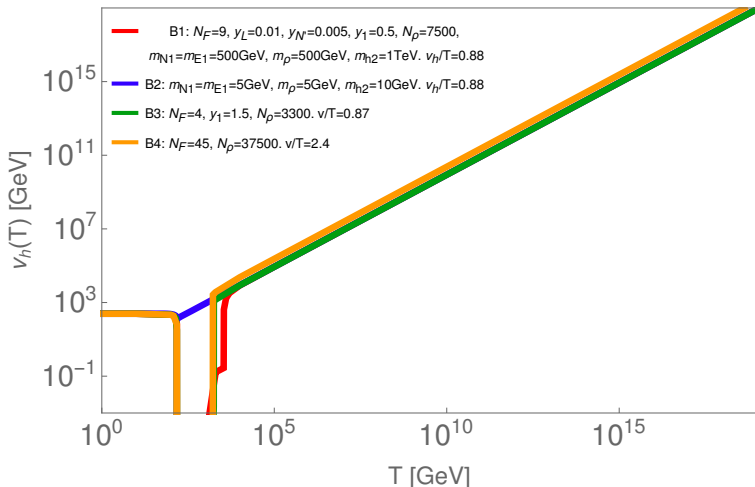


Thermal history in which the electroweak symmetry is always broken.



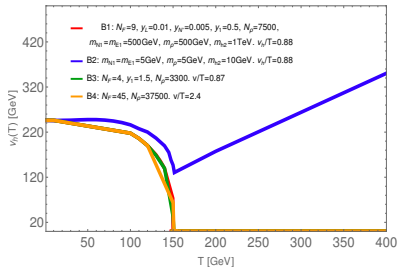
Thermal history in which the electroweak symmetry is only temporarily restored.

THERMAL HISTORIES



Temperature-dependent vev for several benchmarks.

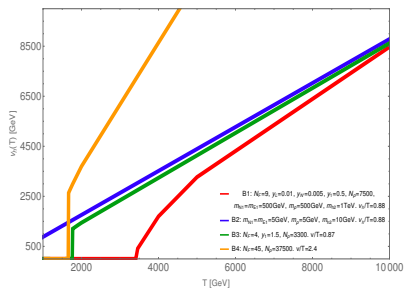
THERMAL HISTORIES



Lower temperature limits of temporary-restored phases.

- B1,B3,B4 have the same lower temperature limits of temporary-restored phases because SM-like Higgs does not couple with new fermions and and new scalars at tree-level.

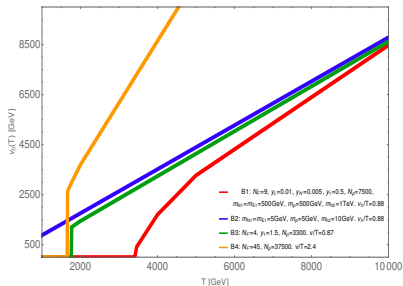
THERMAL HISTORIES



Upper temperature limits of temporary-restored phases.

- The value v_h/T of at high T depends on a_h .

THERMAL HISTORIES



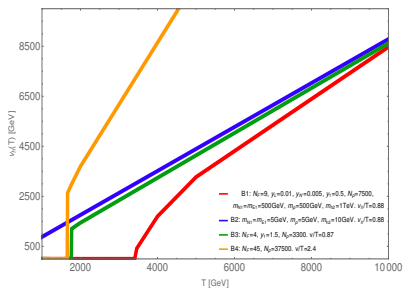
Upper temperature limits of temporary-restored phases.

- The value v_h/T of at high T depends on a_h .

$$\partial_h^2 V_{\text{eff}}(h=0, v_\sigma) \approx -a_h T^2,$$

$$a_h = \frac{N_F}{6y_L} (y_{N'} y_{NN'} y_{NN'2} + y_{E'} y_{EE'} y_{EE'2}) - \left(\frac{3}{16} g^2 + \frac{1}{16} g'^2 + \frac{1}{2} \lambda_2 \right).$$

THERMAL HISTORIES



Upper temperature limits of temporary-restored phases.

- The value v_h/T of at high T depends on a_h .
- The length of temporary-restored phase depends on the masses of new fermions and new scalars (at $T = 0$), $N_\rho \lambda_\rho$, and a_h .

RGES AND STABILITY OF V_{eff}

$$\begin{aligned}
 (4\pi)^2 \frac{d\lambda_2}{dt} &= 24\lambda_2^2 + \frac{3}{8} \left(2g_2^4 + (g_2^2 + g'^2)^2 \right) - (9g_2^2 + 3g'^2) \lambda_2 \\
 &\quad + 2\lambda_3^2 + 2\lambda_3\lambda_4 + \lambda_4^2 + \frac{N_\rho}{2} \lambda_{\rho\Phi_2}^2 + \frac{1}{2} \lambda_{\sigma\Phi_2}^2 \\
 &\quad + 2N_F \left(2 \left(y_{NN'1}^2 + y_{NN'2}^2 + y_{EE'1}^2 + y_{EE'2}^2 \right) \lambda_2 - \left(y_{NN'1}^4 + y_{NN'2}^4 + y_{EE'1}^4 + y_{EE'2}^4 \right) \right)
 \end{aligned}$$

$$(4\pi)^2 \frac{dg'}{dt} = (7 + 2N_F) g'^3$$

$$(4\pi)^2 \frac{dg_2}{dt} = \left(-3 + \frac{2}{3} N_F \right) g_2^3$$

$$\begin{aligned}
 (4\pi)^2 \frac{dy_{NN'1}}{dt} &= 2y_{N'}y_L y_{NN'2} + y_{NN'1} \left[\frac{3}{2} y_{NN'1}^2 - \frac{3}{2} y_{EE'1}^2 + \frac{1}{2} y_{N'}^2 + \frac{1}{2} y_L^2 \right. \\
 &\quad \left. + N_F (y_{NN'1}^2 + y_{NN'2}^2 + y_{EE'1}^2 + y_{EE'2}^2) - \frac{9}{4} g_2^2 - \frac{3}{4} g'^2 \right]
 \end{aligned}$$

$$(4\pi)^2 \frac{d\lambda_\rho}{dt} = 2(N_\rho + 8)\lambda_\rho^2 + \frac{1}{2} \lambda_{\sigma\rho}^2 + 2 \left(\lambda_{\rho\Phi_1}^2 + \lambda_{\rho\Phi_2}^2 \right)$$

RGES AND STABILITY OF V_{eff}

$$(4\pi)^2 \frac{d\lambda_2}{dt} = 24\lambda_2^2 + \frac{3}{8} \left(2g_2^4 + (g_2^2 + g'^2)^2 \right) - (9g_2^2 + 3g'^2) \lambda_2$$

$$+ 2\lambda_3^2 + 2\lambda_3\lambda_4 + \lambda_4^2 + \frac{N_\rho}{2} \lambda_{\rho\Phi_2}^2 + \frac{1}{2} \lambda_{\sigma\Phi_2}^2$$

$$+ 2N_F \left(2 \left(y_{NN'1}^2 + y_{NN'2}^2 + y_{EE'1}^2 + y_{EE'2}^2 \right) \lambda_2 - \left(y_{NN'1}^4 + y_{NN'2}^4 + y_{EE'1}^4 + y_{EE'2}^4 \right) \right)$$

$$(4\pi)^2 \frac{dg'}{dt} = (7 + 2N_F) g'^3, \quad (4\pi)^2 \frac{dg_X}{dt} = -\frac{1}{3} (11N_X - 8n_F) g_X^3$$

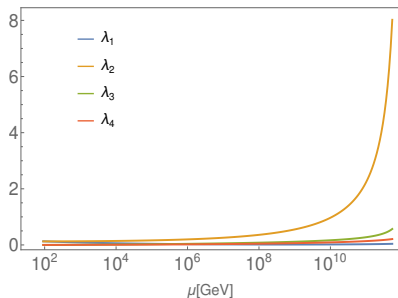
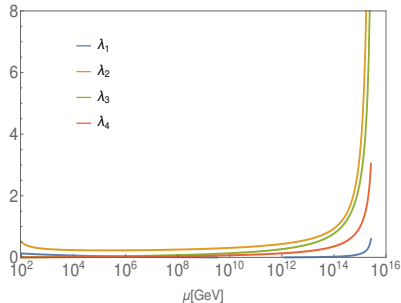
$$(4\pi)^2 \frac{dg_2}{dt} = \left(-3 + \frac{2}{3} N_F \right) g_2^3$$

$$(4\pi)^2 \frac{dy_{NN'1}}{dt} = 2y_{N'} y_L y_{NN'2} + y_{NN'1} \left[\frac{3}{2} y_{NN'1}^2 - \frac{3}{2} y_{EE'1}^2 + \frac{1}{2} y_{N'}^2 + \frac{1}{2} y_L^2 \right.$$

$$\left. + N_F (y_{NN'1}^2 + y_{NN'2}^2 + y_{EE'1}^2 + y_{EE'2}^2) - \frac{9}{4} g_2^2 - \frac{3}{4} g'^2 - 3 \left(N_X - \frac{1}{N_X} \right) g_X^2 \right]$$

$$(4\pi)^2 \frac{d\lambda_\rho}{dt} = 2(N_\rho + 8) \lambda_\rho^2 + \frac{1}{2} \lambda_{\sigma\rho}^2 + 2 \left(\lambda_{\rho\Phi_1}^2 + \lambda_{\rho\Phi_2}^2 \right)$$

(N, N', E, E' ARE CHARGED UNDER $SU(N_X)$. $N_F = N_X n_F$.)

B1: $n_F = 3$, $N_x = 3$.B5: $n_F = 1$, $N_x = 4$.

The effective potential is stable, and the quartic couplings λ_i stays perturbative over a large range of energy scales.

Requiring all couplings stays perturbative up to 10^{10} GeV implies:



$$g' \text{ stays perturbative} \Rightarrow N_F \leq 12$$



$$\lambda_\rho \text{ stays perturbative} \Rightarrow N_\rho \lambda_\rho \lesssim 1.5$$



$$\frac{y_{LV\sigma}}{T} \gtrsim 4, \quad a_\sigma \gtrsim 0, \quad \lambda_\sigma \geq \frac{1}{\lambda_\rho} \left(\frac{\lambda_{\sigma\rho}}{2} \right)^2 \Rightarrow N_\rho \gtrsim \frac{64}{|x_{min}|} N_F$$

x_{min} is the minimum of $f(x) = \frac{\pi^2}{2} x^2 + N_\rho \lambda_\rho J_B(x)$. E.g. choosing $N_\rho \lambda_\rho = 1.5$ implies $N_\rho \gtrsim 552 N_F$.



$$\lambda_2 > 0 \Rightarrow \lambda_2 \gtrsim y_{NN'1}^2 / 2$$

(assume $y_{NN'1} = y_{NN'2} = y_{EE'1} = y_{EE'2}$ at $T = 0$)



$$y_{NN'i}, y_{EE'i} \text{ stays perturbative} \Rightarrow \left(N_X - \frac{1}{N_X} \right) g_X^2 \gtrsim \frac{4}{3} N_F y_{NN'1}^2$$

BENCHMARKS

| | | | | |
|------------------------|-----------------------|-----------------------|-----------------------|-----------------------|
| n_F | 4 | 3 | 3 | 1 |
| N_X | 3 | 3 | 2 | 4 |
| $y_{NN'i} = y_{EE'i}$ | 0.4 | 0.5 | 0.75 | 1.5 |
| $y_{N'}$ | 0.005 | 0.005 | 0.005 | 0.005 |
| $y_{L'}$ | 0.01 | 0.01 | 0.01 | 0.01 |
| $m_{N1}(\text{GeV})$ | 500 | 500 | 500 | 500 |
| N_ρ | 8500 | 7500 | 8500 | 8500 |
| $\lambda_{\sigma\rho}$ | -1.2×10^{-6} | -1.2×10^{-6} | -1.2×10^{-6} | -1.2×10^{-6} |
| λ_2 | 0.081 | 0.126 | 0.28 | 0.54 |
| $m_{h2}(\text{GeV})$ | 1000 | 1000 | 1000 | 1000 |
| $m_\rho(\text{GeV})$ | 500 | 500 | 500 | 500 |
| g_X | 1 | 1.1 | 1.64 | $\sqrt{4\pi}$ |

$$N_\rho \lambda_\rho = 1.5, \quad \lambda_\sigma = \frac{1}{\lambda_\rho} \left(\frac{\lambda_{\sigma\rho}}{2} \right)^2$$

THERMAL EQUILIBRIUM CONDITIONS

- The effective potential at finite temperature above is valid only when N_1 , σ , ρ_i are in thermal equilibrium.

-

$$\Gamma(\rho_i \rho_i \rightarrow \sigma \sigma) \gtrsim H \quad \Rightarrow \quad T \lesssim \frac{\lambda_{\sigma\rho}^2}{\sqrt{N_\rho}} M_{Pl}$$

-

$$\Gamma(N_1 N_1 \rightarrow \sigma \sigma) \gtrsim H \quad \Rightarrow \quad T \lesssim \frac{D_{1\sigma}}{f(m_{N_1}/T)} \frac{y_{11\sigma}^4}{\sqrt{N_\rho}} M_{Pl}$$

$$D_{i\sigma} = \frac{2}{\pi^2} \kappa_i e^{-2\kappa_i} \int_0^\infty dy_1 dy_2 (y_1 + y_1^2/(2\kappa_i))^{1/2} (y_2 + y_2^2/(2\kappa_i))^{1/2} e^{-y_1} e^{-y_2} \int_{-1}^1 d\cos\theta F(\tilde{s})$$

$$F(s) = \left(3s - \frac{25}{16}(s - 1/4)^{-1} - \frac{9}{4} \right) / (8\pi)$$

$$\tilde{s} = s/(4m_i^2) = 1 + (y_1 + y_2)/(2\kappa_i) + y_1 y_2 / (2\kappa_i^2) - (y_1 + y_1^2/(2\kappa_i))^{1/2} (y_2 + y_2^2/(2\kappa_i))^{1/2} \cos\theta / \kappa_i$$

$$\kappa_i = m_{N_i}/T$$

THERMAL EQUILIBRIUM CONDITIONS

- The effective potential at finite temperature above is valid only when N_1 , σ , ρ_i are in thermal equilibrium.

-

$$\Gamma(\rho_i \rho_i \rightarrow \sigma \sigma) \gtrsim H \quad \Rightarrow \quad T \lesssim \frac{\lambda_{\sigma\rho}^2}{\sqrt{N_\rho}} M_{Pl} \sim 100 \text{ TeV}$$

-

$$\Gamma(N_1 N_1 \rightarrow \sigma \sigma) \gtrsim H \quad \Rightarrow \quad T \lesssim \frac{D_{1\sigma}}{f(m_{N_1}/T)} \frac{y_{11\sigma}^4}{\sqrt{N_\rho}} M_{Pl} \sim 100 \text{ TeV}$$

$$D_{i\sigma} = \frac{2}{\pi^2} \kappa_i e^{-2\kappa_i} \int_0^\infty dy_1 dy_2 (y_1 + y_1^2/(2\kappa_i))^{1/2} (y_2 + y_2^2/(2\kappa_i))^{1/2} e^{-y_1} e^{-y_2} \int_{-1}^1 d\cos\theta F(\tilde{s})$$

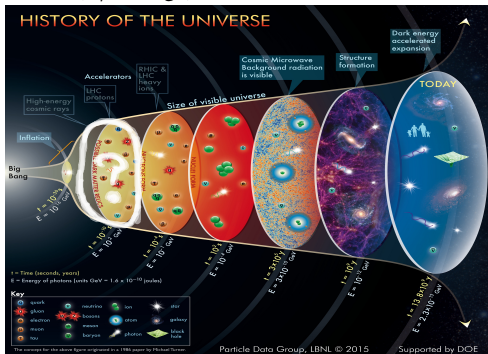
$$F(s) = \left(3s - \frac{25}{16}(s - 1/4)^{-1} - \frac{9}{4} \right) / (8\pi)$$

$$\tilde{s} = s/(4m_i^2) = 1 + (y_1 + y_2)/(2\kappa_i) + y_1 y_2 / (2\kappa_i^2) - (y_1 + y_1^2/(2\kappa_i))^{1/2} (y_2 + y_2^2/(2\kappa_i))^{1/2} \cos\theta / \kappa_i$$

$$\kappa_i = m_{N_i}/T$$

SUMMARY AND OUTLOOK

- EWSNR can be induced by new fermions from renormalizable models.
- The parameter spaces of these models are tightly constrained by theoretical constraints.
- Intriguing cosmological implications: origin of matter-antimatter asymmetry (e.g. high-temperature EWBG), unique gravitational wave signatures, early matter dominated era (N_ρ is large)





EFFECTIVE POTENTIAL

- Effective potential

$$V_{eff} = V_0 + \sum_i \left(V_i^{CW} + V_{1,i}^{th} + V_{ring,i}^{th} \right)$$

- Tree-level potential:

$$V_0 = V_0(\Phi_1, \Phi_2) + V_0(\sigma, \rho) + \tilde{V}_0$$

$$V_0(\Phi_1, \Phi_2) = -\mu_1^2 \Phi_1^\dagger \Phi_1 + \lambda_1 \left(\Phi_1^\dagger \Phi_1 \right)^2 - \mu_2^2 \Phi_2^\dagger \Phi_2 + \lambda_2 \left(\Phi_2^\dagger \Phi_2 \right)^2$$

$$\begin{aligned} \tilde{V}_0 &= \lambda_3 (\Phi_1^\dagger \Phi_1) (\Phi_2^\dagger \Phi_2) + \lambda_4 (\Phi_1^\dagger \Phi_2) (\Phi_2^\dagger \Phi_1) \\ &+ \sum_{i=1}^2 \left(\frac{1}{2} \lambda_{\sigma\Phi_i} \sigma^2 (\Phi_i^\dagger \Phi_i) + \frac{1}{2} \lambda_{\rho\Phi_i} (\rho_i \rho_i) (\Phi_i^\dagger \Phi_i) \right) \end{aligned}$$

$$\begin{aligned} V_0(\sigma, \rho) &= -\frac{1}{2} \mu_\sigma^2 \sigma^2 + \frac{1}{4} \lambda_\sigma \sigma^4 \\ &- \frac{1}{2} \mu_\rho^2 \rho_i \rho_i + \frac{1}{4} \lambda_\rho (\rho_i \rho_i)^2 + \frac{1}{4} \lambda_{\sigma\rho} \sigma^2 \rho_i \rho_i \end{aligned}$$



(Please see hep-ph/9901312 for more details.)

- Coleman-Weinberg potential (for i -th particle)

$$V_i^{CW} = (-1)^{a_i} n_i \frac{m_i^4}{64\pi^2} \left[\log \left(\frac{m_i^2}{\mu^2} \right) - c_i \right]$$

- One-loop thermal potential (for i -th particle)

$$V_{1,i}^{th} = (-1)^{a_i} n_i \frac{T^4}{2\pi^2} J_{B/F} \left(\frac{m_i^2}{T^2} \right)$$

$$J_{B/F}(y^2) = \int_0^\infty dx x^2 \log \left[1 \mp \exp \left(-\sqrt{x^2 + y^2} \right) \right]$$

- Daisy contribution (for i -th particle)

$$V_{ring,i}^{th} = \bar{n}_i \frac{T^4}{12\pi} \left[\left(\frac{m_i^2}{T^2} \right)^{3/2} - \left(\frac{\mathcal{M}_i^2}{T^2} \right)^{3/2} \right]$$



THERMAL CORRECTIONS BEYOND ONE LOOP

$$\begin{aligned}
 V_1^{th}(\phi, T) &= \sum_i \frac{n_i T}{2} \sum_{-\infty}^{\infty} \int \frac{d^3 \vec{k}^2}{(2\pi)^3} \log \left[k^2 + \omega_n^2 + m_i^2(\phi) \right] \\
 &= \sum_i (-1)^{a_i} n_i \frac{T^4}{2\pi^2} J_{B/F} \left(\frac{m_i^2}{T^2} \right)
 \end{aligned}$$

$$V_{ring}^{th}(\phi, T) = \sum_i \frac{\bar{n}_i T}{12\pi} \left[m_i^3(\phi) - \mathcal{M}_i^3(\phi, T) \right]$$

$$\omega_n = 2n\pi T \text{ (bosons)}, (2n + 1)\pi T \text{ (fermions)}$$

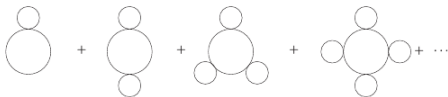


Figure 2: Some generic examples of ring diagrams where each solid line may represent either a scalar, a fermion or a gauge field. The small loops correspond to thermal loops in the IR limit. They are all separately IR divergent, but their sum is IR finite.



$\mathcal{M}_i^2(\phi, T) = m_i^2(\phi) + \Pi_i(\phi, T)$ (except $i = Z_L, \gamma_L$).

Truncated Full Dressing Method:

$$\begin{aligned} \Pi_h(\phi, T) &= \left(\frac{3g^2 + g'^2}{16} + \frac{\lambda}{2} + \frac{y_t^2}{4} \right) T^2 = \Pi_\chi(\phi, T) , \\ \Pi_{W_L}(\phi, T) &= \frac{11}{6} g^2 T^2 , \\ \Pi_{W_T}(\phi, T) &= \Pi_{Z_T}(\phi, T) = \Pi_{\gamma_T}(\phi, T) = 0 , \quad (\text{A14}) \\ \mathcal{M}_{Z_L}^2(\phi) &= \frac{1}{2} \left[m_Z^2(t) + \frac{11}{6} \frac{g^2}{\cos^2 \theta_W} T^2 + \Delta(\phi, T) \right] , \\ \mathcal{M}_{\gamma_L}^2(\phi) &= \frac{1}{2} \left[m_Z^2(t) + \frac{11}{6} \frac{g^2}{\cos^2 \theta_W} T^2 - \Delta(\phi, T) \right] , \end{aligned}$$

(A15)



Optimized Partial Dressing Method:

$$\delta m_{\phi_j}^2(h, T) = \sum_i \frac{\partial}{\partial \phi_j} \left[\frac{\partial V_{\text{CW}}^i}{\partial \phi_j} (m_i^2(h) + \delta m_i^2(h, T)) + \frac{\partial V_{\text{th}}^i}{\partial \phi_j} (m_i^2(h) + \delta m_i^2(h, T), T) \right] \quad (\text{A.1})$$

$$\delta m_j^2(h, T) \approx \delta m_{j(a)}^2 + (h - h_a) \frac{\partial \delta m_{j(a)}^2}{\partial h} \quad (\text{A.2})$$

$$V_{\text{eff}}^{\text{pd}}(h, T) = V_0 + \sum_i \int dh \left[\frac{\partial V_{\text{CW}}^i}{\partial h} (m_i^2(h) + \delta m_i^2(h, T)) + \frac{\partial V_{\text{th}}^i}{\partial h} (m_i^2(h) + \delta m_i^2(h, T), T) \right], \quad (\text{A.4})$$



DAISY AND SUPER-DAISY CONTRIBUTIONS TO THERMAL MASS

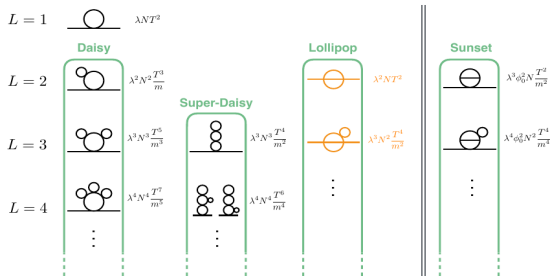


Figure 2. Complete set of 1- and 2-loop contributions to the scalar mass, as well as the most important higher loop contributions, in ϕ^4 theory. The scaling of each diagram in the high-temperature approximation is indicated, omitting symmetry- and loop-factors. Diagrams to the right of the vertical double-lines only contribute away from the origin when $\langle \phi \rangle = \phi_0 > 0$. We do not show contributions which trivially descend from e.g. loop-corrected quartic couplings. Lollipop diagrams (in orange) are not automatically included in the resummed one-loop potential.



V_{eff} IN SM

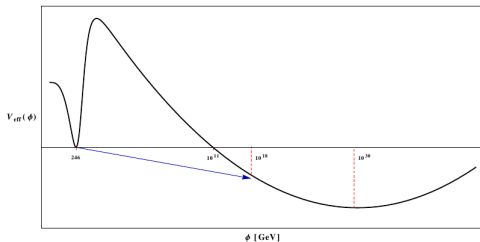


FIG. 2: The potential in the Standard Model, for $M_H = 125.7$ GeV and $M_t = 173.34$ GeV, is sketched (figure not to scale). The potential goes negative at a scale of 10^{11} GeV and reaches a new minimum at roughly 10^{30} GeV. The tunneling through the barrier goes from the base of the arrow ($\phi(r = \infty)$) to the tip ($\phi(0)$), which turns out to be close to or above the Planck scale.

Branchina, Messina & Sher, arXiv:1408.5302



STABILITY OF V_{eff} IN SM AND SINGLET-DOUBLET MODEL

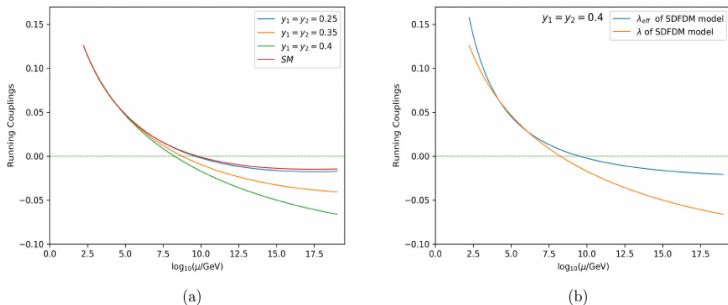
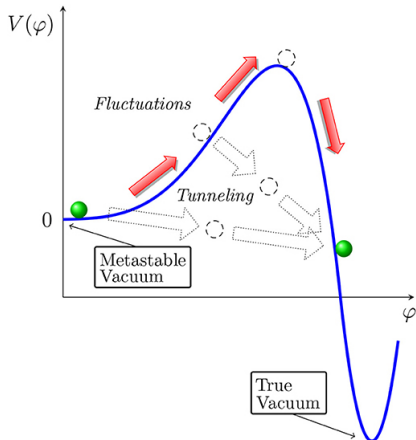


FIG. 1. (a) $\lambda(t)$ up to M_{Pl} for the SM and for various Yukawa couplings in the SDFDM model; (b) Running $\lambda(t)$ and $\lambda_{eff}(t)$ up to M_{Pl} scale for the SDFDM model.



METASTABLE VACUUM VS TRUE VACUUM





In SM:

$$\tau = \left[\frac{R_M^4}{T_U^4} e^{\frac{8\pi^2}{3|\lambda(\mu)|}} \right] \times [e^{\Delta S}] \times T_U$$

$$R_M \sim 1.87 \cdot 10^{-17} \text{ GeV}^{-1} = 224.5 M_P^{-1}$$

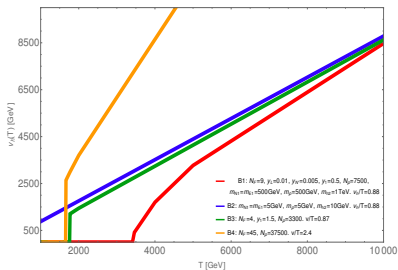
$$\lambda(1/R_M) = -0.01345,$$

$$\tau_{tree} \sim 10^{613} T_U$$



$$(4\pi)^2 \frac{d\lambda_1}{dt} = 24\lambda_1^2 - 6y_t^4 + \frac{3}{8} \left(2g_2^4 + (g_2^2 + g'^2)^2 \right) + (12y_t^2 - 9g_2^2 - 3g'^2) \lambda_1 \\ + 2\lambda_3^2 + 2\lambda_3\lambda_4 + \lambda_4^2 + \frac{N_\rho}{2} \lambda_{\rho\Phi_1}^2 + \frac{1}{2} \lambda_{\sigma\Phi_1}^2$$

$$(4\pi)^2 \frac{dg_3}{dt} = -7g_3^3$$



Upper temperature limits of temporary-restored phases.

Table 1. Frequency classification of gravitational waves and their detection method [4-6]

| Frequency band | Detection method |
|---|--|
| Ultra high frequency band: above 1 THz | Terahertz resonators, optical resonators, and magnetic conversion detectors |
| Very high frequency band: 100 kHz–1 THz | Microwave resonator/wave guide detectors, laser interferometers and Gaussian beam detectors |
| High frequency band (audio band)*: 10 Hz–100 kHz | Low-temperature resonators and ground-based laser-interferometric detectors |
| Middle frequency band: 0.1 Hz–10 Hz | Space laser-interferometric detectors of arm length 100 km – 60,000 km, atom and molecule interferometry, optical clock detectors |
| Low frequency band (milli-Hz band): 100 nHz–0.1 Hz | Radio Doppler tracking of spacecraft, space laser-interferometric detectors of arm length longer than 60,000 km, optical clock detectors |
| Very low frequency band (nano-Hz band): 300 pHz – 100 nHz | Pulsar timing arrays (PTAs) |
| Ultralow frequency band: 10 fHz–300 pHz | Astrometry of quasars and their proper motions |
| Extremely low (Hubble) frequency band (cosmological band): 1 aHz–10 fHz | Cosmic microwave background experiments |
| Beyond Hubble-frequency band: below 1 aHz | Through the verifications of inflationary/primordial cosmological models |

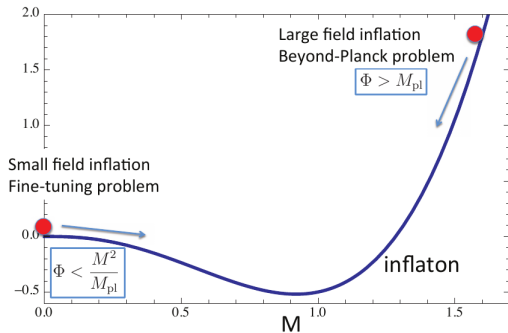
*The range of audio band (also called LIGO band) normally goes only to 10 kHz.

†The range of milli-Hz band is 0.1 mHz to 100 mHz.

arXiv:1709.05659



SLOWLY-ROLLING SCALARS



Iso, Kohri & Shimada, arXiv:1511.05923